The small crater Heinsius A which exhibited the radar enhancement is the bright spot indicated by the arrow.

Also, it is known that during a lunar eclipse the rayed craters exhibit a different cooling rate than the rest of the lunar surface. The most recent measurements of a lunar eclipse in December 1964, show that many other craters also show this anamolous cooling behavior. One of the newly discovered "thermal-anamolous" craters has been tentatively identified as Heinsius A, the crater which was bright under full moon and showed a radar enhancement. The optical, thermal, and radar results can be explained by localized areas of bare, exposed, and compact rock.

In conclusion, lunar radar echoes were examined in delay and frequency in a manner such that returns were reflected from localized areas on the lunar surface. The mapping of these returns showed that young and rayed craters have enhanced radar scattering. The craters which show these radar enhancements always appear bright on the full moon and from the latest infrared results, appear to be anamolous in that regime also. The results at all wavelengths can be explained if these are localized areas of bare, exposed, and compacted rocks.

Although this paper concerned the radar behavior of young and rayed craters it should be noted that the mountainous regions were shown to reflect more power than the maria regions. The enhancements were much less modest than those for the craters. For example, mountainous regions reflected 1½ to 2 times as much power as the maria region, while scattering enhancements of craters show they reflected up to 10 or 20 times as much power as other areas on the moon.

Discussion Following Thompson's Paper

T. Hagfors: What reflection law did you use?

T. W. Thompson: An empirical law based on observation from Millstone Hill at 440 Mc/s, using a 100-μsec pulse length.

C. Sagan: Have you looked to see whether there is any systematic difference between the scattering behavior of craters without central peaks?

T. W. Thompson: I have not looked specifically for this effect.

C. Sagan: Such a correlation might be expected.

(Paper 69D12–620)

Interpretation of the Angular Dependence of Backscattering From the Moon and Venus

Petr Beckmann

Electrical Engineering Department, University of Colorado, Boulder, Colo.

and

W. K. Klemperer

Central Radio Propagation Laboratory, National Bureau of Standards, Boulder, Colo.

A previously derived formula, expressing the variation of the mean power backscattered from the rough surface of a planet with the delay time or angle of incidence by taking into account both the composite roughness of the surface and shadowing effects, is checked against new data from the Moon and Venus at five different wavelengths. The agreement with the lunar data is very good and leads to certain conclusions on the nature of the lunar surface. The data on Venus are also in good agreement and indicate that its surface is smoother than that of the Moon, but with an abundance of small structure.

1. Introduction

The problem of extracting information on the lunar and planetary surfaces from the measurements of radar backscatter from these surfaces has been the subject of many studies in recent years [cf. bibliography given by Evans, 1965a]. Until recently, no theory free of arbitrary and unnatural assumptions could provide a fit to the measured curves of backscattered power versus delay time (i.e., angle of incidence) and in the absence of this basic agreement the conclusions drawn from the measured curves must necessarily be doubtful.

In the present paper we hope to show that very good agreement with the measured curves may be obtained over the entire range of delay time by applying basic Kirchhoff theory and refining it to include two important effects: composite roughness and shadowing.

For radar backscatter from the Moon or a planet the pertinent geometry may be seen from figure 1. A radio pulse of duration T_P traveling with velocity c illuminates an annular ring of area A on the surface of the planet. This area is easily shown independent of position and equal to $A=2\pi acT_p$ with a the radius of the planet. The angle of incidence θ changes from 0° to 90° as the pulse travels from the subterrestrial

786–228 O–66–12

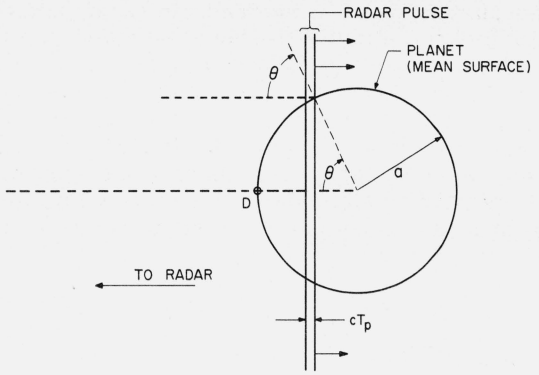

FIGURE 1. *Geometry of radar backscatter from a planet.*

point D to the limbs of the planet; for sufficiently short pulse durations T_p (or equivalent techniques of attaining high resolution), θ remains essentially constant over the illuminated area. The radar will measure the mean backscattered power P^* as a function of the delay time t; we set $t=0$ when the pulse first reaches the point D. It will be seen from figure 1 that θ is a simple function of the delay time t:

$$\theta=\arccos\,(1-ct/2a). \tag{1}$$

Using (1), the measured curve $P^*(t)$ is easily plotted as a function of θ and, to permit comparison under varying conditions of equipment, etc., is normalized to the "angular spectrum" by dividing by P^* for $\theta=0$, i.e.,

$$P(\theta)=\frac{P^*(\theta)}{P^*(0)}. \tag{2}$$

It is against this experimentally measured function that a theoretically derived function $P(\theta)$ must be checked before any conclusions on the nature of the planetary surface can be drawn.

2. Theory

There is at present no general theory leading to explicit results for electromagnetic scattering by *any* kind of a rough surface $\xi(x, y)$ where ξ is the deviation from a (mean) xy plane, the surface being the interface between two regions of arbitrary electrical constants. However, the solution is available [Beckmann and Spizzichino, 1963] for a large class of surfaces, including those generated by a stationary random process $\xi(x, y)$; this class is limited by the following assumptions: (a) the surface bounds a perfectly conducting region, (b) the radii of curvature of the surface are large compared to the wavelength, i.e., the surface does not have an abundance of sharp points or edges, and (c) multiple scattering may be neglected.

Assumption (a) seems at first sight unrealistic for lunar or planetary surfaces, and so it doubtless is if only the conductivity *per se* is considered. However, all experimental and theoretical evidence indicates that for the scattering characteristics of a surface, the roughness is much more significant than the conductivity: a change in conductivity may change the scale of the scattering diagram, but will not—like a change in roughness or slopes—significantly change its shape and general character. On the other hand, the above statements concern only the amplitude and power scattering characteristics (mean or random); they certainly do not apply to problems of depolarization, which can be shown to be very strongly dependent on conductivity, and permittivity. In fact, the theory to be outlined below is not suited for direct application to problems of depolarization and we shall not attempt to solve them in this paper.

Under the above assumptions one may derive the field scattered into an arbitrary direction (e.g., the backscatter direction) when the surface is illuminated by a plane wave at an angle of incidence θ. In the case of interest here, namely when $\xi(x, y)$ is generated by an isotropic stationary process with probability density $p(z)$ and correlation function

$$B(\tau)=<\xi(x_1, y_1)\xi(x_2, y_2)>, \tag{3}$$

with τ the distance between the points (x_1, y_1) and (x_2, y_2) on the mean (smooth) surface, the solution is derived in chapter 5 of Beckmann and Spizzichino [1963].

When the above procedure is applied to the case of backscatter for the geometry of figure 1, the agreement with the measured curves (2) is closest if $p(z)$ is normal (mean 0, variance σ_1^2) and the correlation function (3) is exponential:

$$B(\tau)=\sigma_1^2 e^{-|\tau|/T_1}, \tag{4}$$

where the constant T_1 is the correlation distance, i.e., the value of τ for which $B(\tau)=e^{-1}$. For the above functions $p(z)$ and $B(\tau)$ one obtains [Beckmann, 1965a]

$$P_0(\theta)=\left(\cos^4\theta+\frac{\lambda^2 T_1^2}{16\pi^2\sigma_1^4}\sin^2\theta\right)^{-3/2}, \tag{5}$$

with λ the wavelength of the incident radiation.

However, the agreement of (5) with the measured dependence $P(\theta)$ is not satisfactory for two reasons: (a) The value of T_1^2/σ_1^2 for which the best agreement is obtained is unrealistically high, i.e., far off the values to be expected from optical observations of the lunar surface, (b) agreement is obtained only over the range of θ from 0° to about 60°, but not near the limbs, where the measured "tail" of the echo falls off rapidly as θ approaches 90°, whereas (5) approaches a constant value.

The theory was therefore refined in two respects. The first [Beckmann, 1965a] concerns an analysis of a rough surface generated by a superposition of several random processes:

$$\xi(x, y)=\xi_1(x, y)+\xi_2(x, y)+\ldots+\xi_n(x, y), \tag{6}$$

each with its own distribution and correlation function. Let the distributions of the ξ_j be normal with mean zero and variances σ_j^2, so that the scale roughness of the jth component $\xi_j(x, y)$ is

$$r_j = \frac{\sigma_j}{\lambda}, \tag{7}$$

and let the correlation function of this component be

$$B_j(\tau) = \sigma_j^2 e^{-|\tau|/T_j} \tag{8}$$

so that its "equivalent" root-mean-square slope is [1]

$$s_j = \sqrt{\lim_{\tau \to 0} |B''(\tau)|} = \frac{\sigma_j}{T_j}. \tag{9}$$

It can then be shown [Beckmann, 1965a] that instead of (5) we obtain the more general expression

$$P_0(\theta) = (\cos^4 \theta + R \sin^2 \theta)^{-3/2}, \tag{10}$$

where

$$R = \frac{1}{\left(4\pi \sum_{j=1}^{n} r_j s_j\right)^2}. \tag{11}$$

For a given wavelength, R is a constant and thus (10) has the same form as (5); however, owing to Cauchy's inequality,

$$\left(\sum_j r_j s_j\right)^2 \leq \sum_j r_j^2 \sum_j s_j^2 = r^2 s^2, \tag{12}$$

the numerical value of R, now a result of summing many components, is reasonable when interpreted in terms of scale roughness and rms slope of the surface. It should be noted from (11) that (10) will be strongly affected not only by the roughness r_j of the individual components, but also by their slopes s_j, which stresses the importance of small-scale components.[2]

Curves of (10) for various values of R are shown in figure 2.

The second refinement of the theory, which corrects the disagreement of (10) with the measured dependence near the limbs, concerns partial shadowing of the rough surfaces. It is usually assumed in calculations of rough-surface scatter that all parts of the surfaces are illuminated. In reality this is only true for normal incidence ($\theta = 0°$); for other values of θ the hills will cast shadows on other parts of the surface (fig. 3). These parts of the surface will not be effective in scattering. The power backscattered by a partially shaded surface may be calculated by determining the statistical characteristics of the surface consisting of the illuminated parts of the original surface only. This has been done elsewhere [Beck-

[1] A random process with correlation function (8) does not have an rms slope: the quantity s_j is defined by (9) and is named "equivalent" rms slope for reasons evident from its derivation [Beckmann, 1965a]. This is done here to avoid certain mathematical issues of secondary importance.

[2] Relations (10) and (11) hold if the components in (6) are independent. If this is not so, cross-correlation functions must be considered, which leads to more involved mathematics, but not to changes in principle [cf. Hayre, 1965].

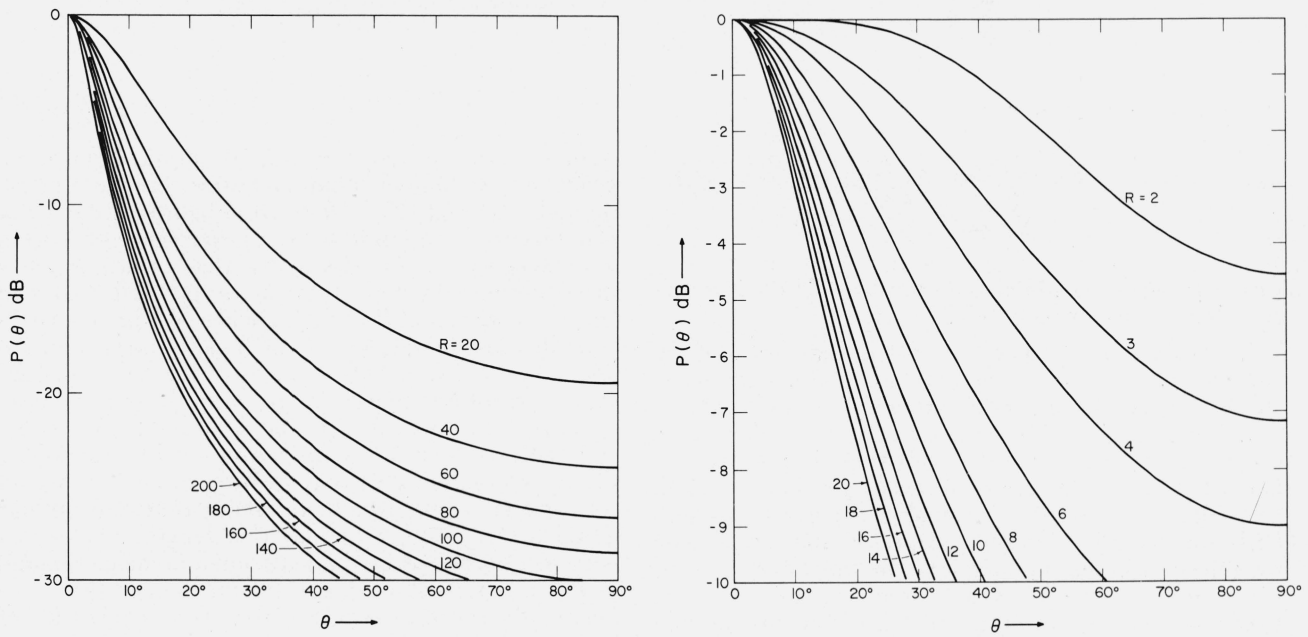

FIGURE 2. *Mean relative backscattered power as given by (10) for various values of* R.

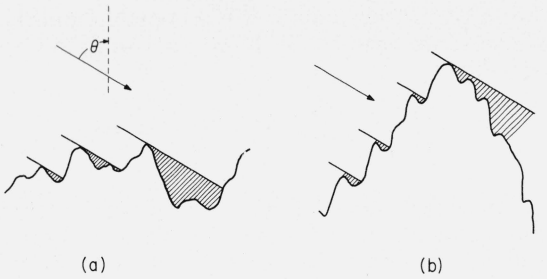

FIGURE 3. *Shadowing of a rough surface, (a) general, (b) effect of small structure.*

mann, 1965b] and leads to a shadowing function $S(\theta)$ which yields the mean backscattered power for a partially shaded surface through

$$P(\theta) = S(\theta)P_0(\theta), \tag{13}$$

where $P_0(\theta)$ is the backscattered power calculated without regard to shadowing, e.g., (10).

In the special case of a normally distributed surface, the shadowing function reduces to [Beckmann, 1965b]

$$S(\theta) = \exp\left[-\frac{1}{4}\tan\theta \operatorname{erfc}(K\cot\theta)\right], \tag{14}$$

where

$$\operatorname{erfc} x = 1 - \operatorname{erf} x = \frac{2}{\sqrt{\pi}}\int_x^\infty e^{-t^2}dt, \tag{15}$$

and the constant K is given by

$$K = \frac{1}{\sqrt{2|B''(0)|}}, \tag{16}$$

or in the case of (6) and (8) by

$$K = \frac{1}{\sqrt{2\sum_{j=1}^{n} s_j}} = \frac{1}{s\sqrt{2}}, \tag{17}$$

with s_j given by (9) and hence s the overall "equivalent" rms slope of the surface (see footnote 1).

It should again be noted that it is the slopes of the surface that determine the extent of shadowing, since $|B''(0)|$ equals the mean square slope of the surface; thus it may again be the small-scale components (small roughness r_j) that are decisive if their slopes are sufficiently large. The physical reason for this is evident from figure 3b, where the small-scale variations partially shade the "south" slope of the large-scale roughness without adding light to the "north" side.

Curves of (14) with K as parameter are shown in figure 4. The shadowing functions $S(\phi)$ are plotted in decibels so as to facilitiate multiplication by the curves of $P_0(\theta)$ in figure 2.

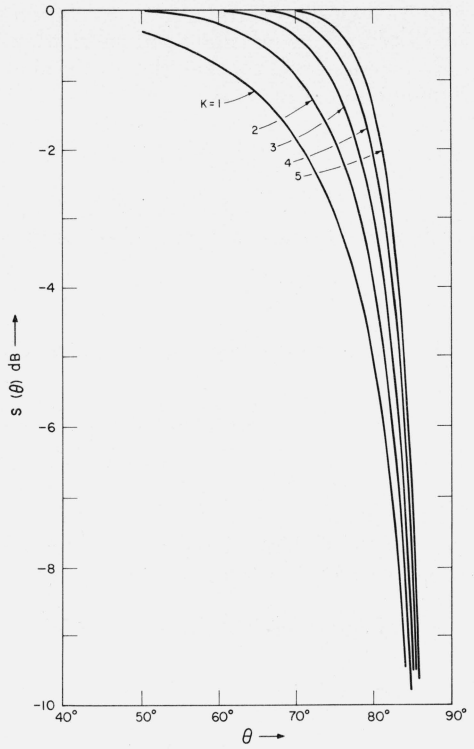

FIGURE 4. *Shadowing function S(θ) given by (14) for various values of* K.

From (10), (13), and (14) we obtain our final formula for the mean relative power backscattered from the lunar or Venusian surface as a function of the angle of incidence,

$$P(\theta) = (\cos^4\theta + R\sin^2\theta)^{-3/2}\exp\left[-\frac{1}{4}\tan\theta \operatorname{erfc}(K\cot\theta)\right], \tag{18}$$

where K and R are meaningful physical constants given by statistical characteristics of the surface through (11) and (17). Note from figures 2 and 4 that R determines the curve for the lower range of θ, while K determines it near the limbs; thus in fitting (18) to the experimental data, there is no possibility of arbitrary adjustment of R at the expense of K or vice versa.

In the rest of this paper we hope to show that (18) does indeed give a very good fit to the data available to us. However, before we go on to the experimental curves, it is well to realize that R and K are constants only with respect to θ; in general they are functions of the wavelength. This may be seen immediately from (11) and (7), from which it follows that R is proportional to λ^2. This principal wavelength dependence is in fact borne out by the experimental measurements made at different frequencies: the longer the wavelength, the more peaked the response near $\theta = 0°$ (cf. figs. 5 and 6).

However, apart from this principal and explicit

wavelength dependence, there are other frequency-dependent factors which are not as easily determined quantitatively. Of these, two appear most important. First, let us write (6) in decreasing orders of σ_j; the components with $\sigma_j << \lambda$ will obviously have no effect (or the same effect as $\xi_j \equiv 0$) on the backscattered power, e.g., local facets of the surface that reflect radio frequencies specularly may be rough on an optical scale. Thus n in (6) is, in effect, frequency-dependent and hence by (11) and (17) R and K must also be frequency-dependent. Secondly, the shadowing function (14) was derived from purely geometrical considerations; the penumbral regions caused by diffraction were neglected. Since diffraction is a frequency-dependent phenomenon, this is a further reason why K must be frequency-dependent. The error in neglecting diffraction will appear as a distorted numerical value of K as determined through (17); this part of the error will vanish as $\lambda \rightarrow 0$.

These secondary, implicit frequency-dependencies are in fact borne out in the numerical values of R and K even when the explicit dependence of R on λ^2 has been accounted for, as we shall see in the following sections.

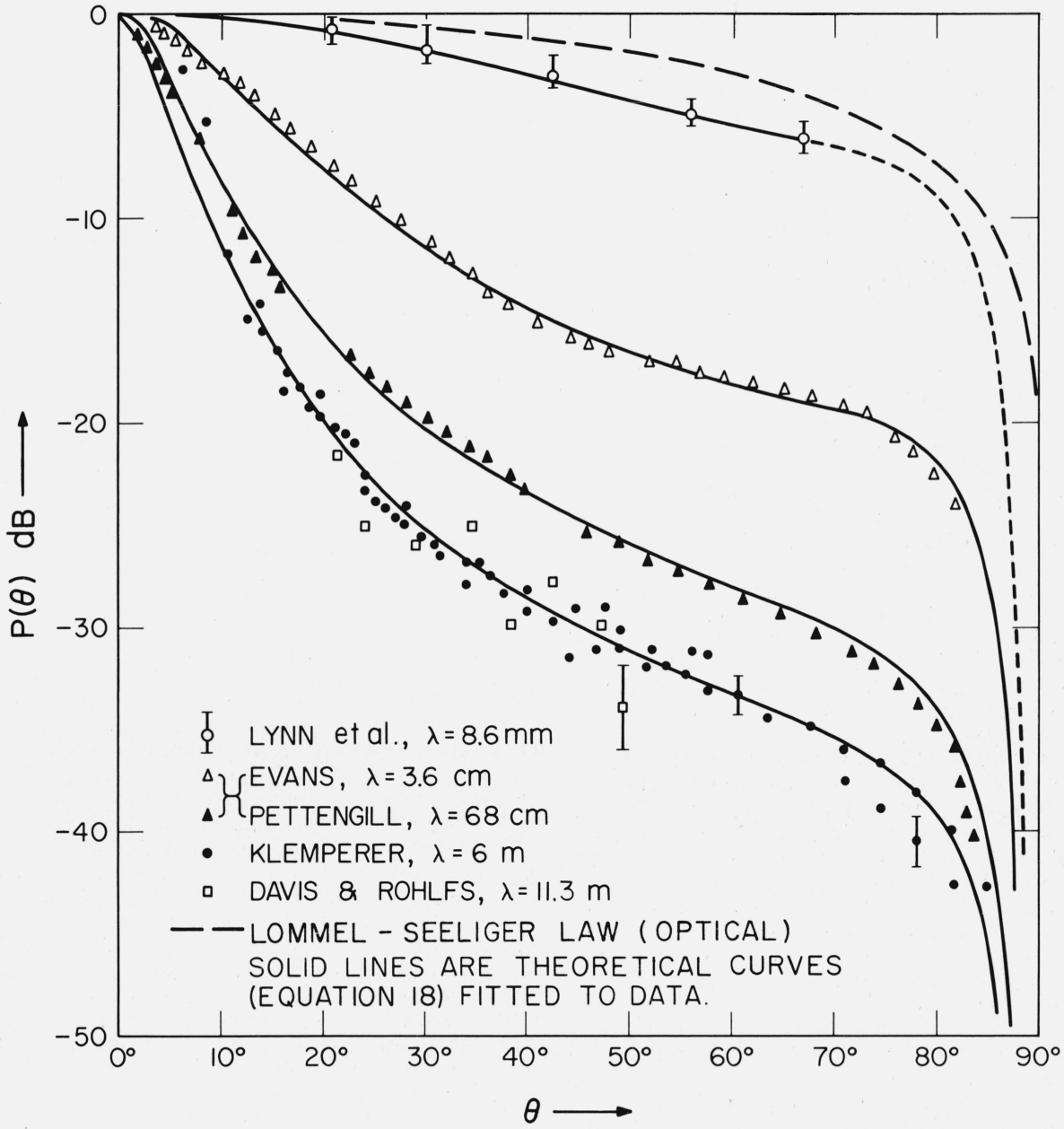

FIGURE 5. *Comparison of (18) with lunar radar data measured at five different wavelengths.*
The optical data follow from the uniform brightness of the lunar disk.

3. The Moon

For a convincing check of (18) against the experimental lunar data, the measured curve $P(\theta)$ should be known over a sufficiently wide range of θ; otherwise the fit is obtained too easily to provide a reliable verification of the theory. The high-resolution lunar backscatter measurements over a sufficiently wide range of θ that are available to us are those made at wavelengths of 8.6 mm, 3.6 cm, 68 cm and 6 m as reported below.

Lynn, Sohigian, and Crocker [1964], using a radar located at Lexington, Mass., at 34,990 Mc/s (8.6 mm) with a power of 12 W and a beamwidth of 4.3 min of arc, measured values of $P(\theta)$ shown in figure 5 together with the curve computed from (18). A close fit is obtained for $R=3$ and K in the neighborhood of 4; their measurements do not go far enough out to the limbs to determine K more accurately.

A better check on (18) is provided by the data reported by Evans and Pettengill [1963] for $\lambda=3.6$ cm and 68 cm. The measurements at 3.6 cm were made with a radar located at Pleasanton, Calif., with 12 kW peak power with a resolution of 30 μsec. The resulting data are again shown in figure 5, together with the curve computed from (18) for $R=21$, $K=3.6$. It will be seen that the curve fits the measured dependence to within 1 dB.

The next set of data in figure 5 is the one measured by Evans and Pettengill [1963] with a 440-Mc/s (68-cm) radar located at Westford, Mass. Using a power of 2 MW, a resolution of 12 μsec was attained. Because of the high resolution of these measurements and the range in θ (almost to 90°), this set of data is of the highest quality and ampleness presently available. As may be seen from the figure, (18) again provides an extremely close fit for $R=85$ and $K=0.95$.

The squares in figure 5 show the data obtained by Davis and Rohlfs [1964] at a wavelength of 11.3 m using 250-μsec pulses; a fit to these data is obtained for $R=200$. The measurements do not go out far enough to the limbs to determine a value for K; also, the relatively large scatter and error bars make accurate comparison difficult.

Finally, figure 5 shows the data on $P(\theta)$ obtained at $\lambda=6$ m (49.92 Mc/s) by Klemperer [1965] using the radar at Jicamarca, Peru, with a power of 2 MW and resolution of 100 μsec. The solid line computed from (18) for $R=165$ and $K=0.03$ once more yields a very good fit to the measured data.

Also indicated in figure 5 (top curve) is the Moon's uniform brightness at optical sequence as given by Lommel-Seeliger law [Evans, 1965a, p. 35]. Formula (18) matches this curve for $R\sim 2$, $K\sim 5$.

As expected, R and K turn out to be frequency-dependent. Figure 6 shows an attempt to plot the functions $K(\lambda)$ and $R(\lambda)$. Although we certainly do not claim these curves—given by only four points each—to be the exact dependencies, the figure leaves little doubt that the values of K and R, originally picked to give the closest fits in figure 5, are not accidental, but follow a monotonic pattern consistent

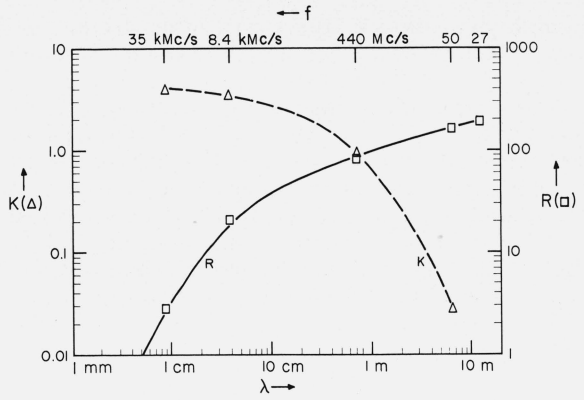

FIGURE 6. *Dependence of* R *and* K *on wavelength for the lunar surface.*

with the discussion at the end of the preceding section: on the longer wavelengths, diffraction will be more effective and will thus reduce the shadowing effect (compare the dependence on K in fig. 4). Similarly, the values of $R(\lambda)$ appear to lie on a smooth, monotonic curve; for the reasons given in the preceding section, R is an increasing function of the wavelength.

Relation (17) was derived by geometrical optics and will therefore be strictly valid only as $\lambda\to 0$. For the shortest wavelengths available, 8.6 mm [Lynn, Sohigian, and Crocker, 1964] and 3.6 cm [Evans and Pettengill, 1963], K will be seen from figure 6 to lie in the neighborhood of 4, which by (7) corresponds to an effective rms slope of the lunar surface of 10°. However, for the reasons given above, this value should be used with caution.

4. Venus

The experimental data that are available in sufficient detail to permit a check of (18) are those by Dyce, Pettengill, and Sanchez [1965], Kotelnikov [1965], and Evans [1965b]. In addition, the angular characteristic may be inferred from the frequency spectrum reported by Carpenter [1964] and Muhleman [1965] or from the power-delay time curve obtained with a long pulse [Klemperer, Ochs, and Bowles, 1964].

Figure 7 shows the data measured by Dyce, Pettengill, and Sanchez [1965] at the Arecibo Ionospheric Observatory at 430 Mc/s (70 cm). The full curve is a plot of (18) for $R=120$, $K=1.0$. The theoretical curve is seen to be generally in good agreement with the measured data, although an irregularity appears in the range from about 20° to 50°; a similar irregularity appears in figure 9 in a different position, and might therefore be attributed to a large inhomogeneity of the surface (e.g., continents) presenting different aspects to the terrestrial radar at different times owing to Venus's rotation [Carpenter, 1965].

Figure 8 shows the data measured in the USSR in 1962 (upper curve) and 1964 (lower curve) at a wave-

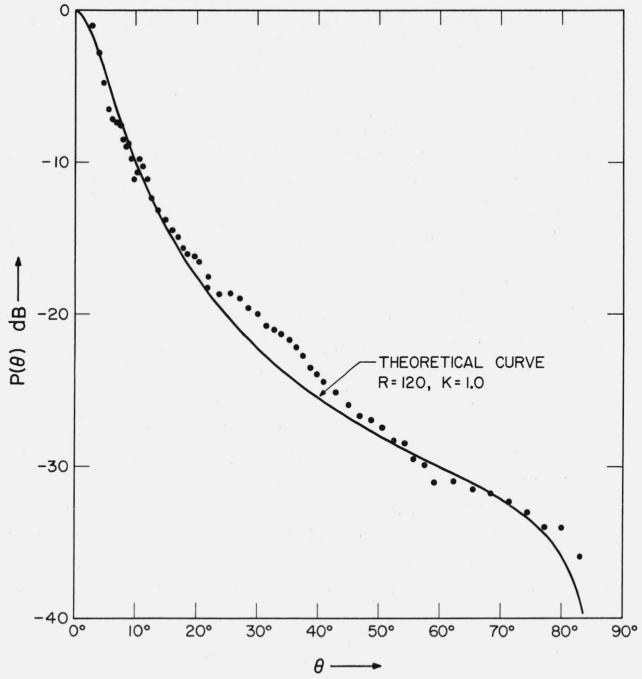

FIGURE 7. *Comparison of (18) with data measured at 70 cm for Venus [Dyce, Pettengill, and Sanchez, 1965].*

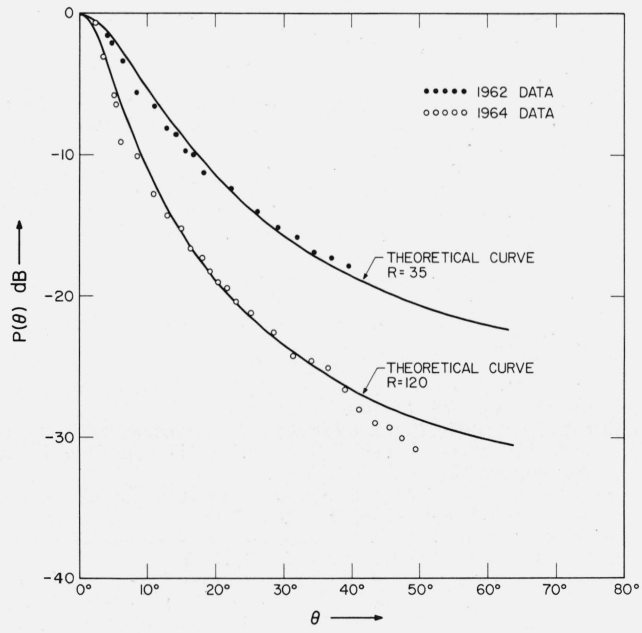

FIGURE 8. *Comparison of (18) with the data measured at 43 cm for Venus [Kotelnikov, 1965].*

length of 43 cm as reported by Kotelnikov [1965]. The full curves plot (18) for $R=35$ and 120 respectively. Kotelnikov [1965] attributes the difference in the two sets of measurements to a smoother side of Venus being turned to the Earth during the 1964 measurements; however, no such difference is apparent in the JPL data [Carpenter, 1964; Muhleman, 1965],

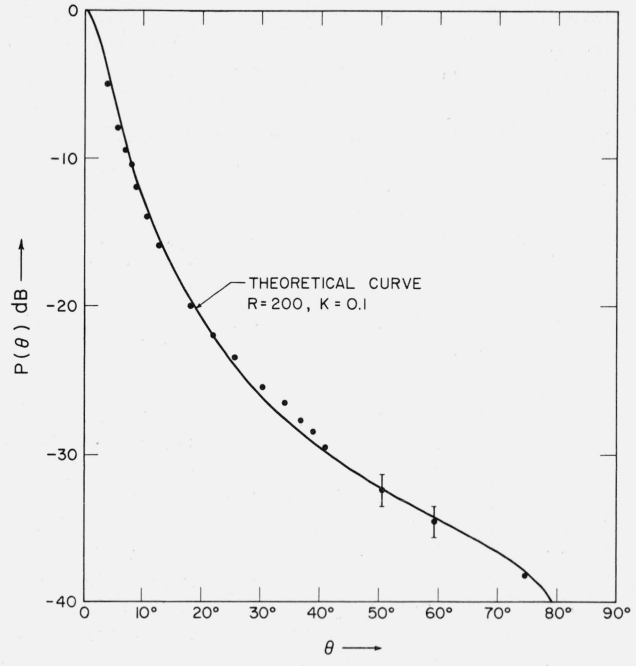

FIGURE 9. *Comparison of (18) with data measured at 23 cm for Venus [Evans, 1965b].*

which were also taken in 1962 and 1964 at a different wavelength (12.5 cm). Also, the value $R=35$, which provides a fit to the 1962 data, is far lower than any corresponding to any other set of measurements, and we are therefore inclined to give more weight to the 1964 USSR data, which are consistent with all the rest of the data which we have investigated.

Figure 9 shows the data obtained by Evans [1965b] at a wavelength of 23 cm. A very good fit is obtained from (18) for $R=200$, $K=0.1$.

Additional values for the parameter R and some estimates for K can be obtained from the data available at $\lambda=12.5$ cm and $\lambda=6$ m. A curve of $P(\theta)$ versus θ was obtained by Carpenter [1964] from a CW radar spectrum of Venus taken on December 5, 1962, by inverting an integral equation. The radar was operated at 8350 Mc/s with a power of 12 kW. Values of $R\sim 140$ and $K\sim 0.4$ are appropriate in fitting equation (18) to these data, although the scatter in the points beyond $\theta=30°$ is considerable. The same radar was used again in 1964 (near closest approach to Venus) but with an increase in CW transmitter power to 100 kW. A very fine spectrum was obtained on June 17 [D. O. Muhleman, private communication], from which a value of $R=120$ can be inferred for the backscatter function. The data at $\lambda=6$ m [Klemperer, Ochs, and Bowles, 1964] were obtained with the Jicamarca radar in Peru using 500-μsec pulses. Only an estimate of the true $P(\theta)$-versus-θ curve can be made, as convolution effects are serious. Independent estimates of the value for R were also obtained from (a) the spectrum of fading, (b) the comparison of echo amplitude on 3-msec and 500-μsec

pulses. The value for the parameter R thus found is 200 ± 50. All the data available from $\lambda = 6$ m to $\lambda = 12.5$ cm are summarized in table 1.

TABLE 1. *Values of* R *and* K *for Venus.*

$f_{Mc/s}$	λ	R	K	Exp date	References
50	6 m	~ 200		12/2/62	Klemperer, Ochs, and Bowles [1964].
430	70 cm	120	1.0	5/22/64	Dyce, Pettengill, and Sanchez [1965].
700	43 cm	~ 35		1962	Kotelnikov [1965].
		120		1964	
1295	23 cm	200	0.1	1964	Evans [1965b].
8350	12.5 cm	~ 140	~ 0.4	12/5/62	Carpenter [1964].
		~ 120		6/17/64	Muhleman (private communication).

It will be seen from figures 7 to 9 that again (18) is in good agreement with the measured dependencies. The values of K are now less reliable than in the case of the Moon, since the measurements taken from Venus, particularly at the shorter wavelengths, do not go out to the limbs far enough. The values of R do not vary with wavelength as strongly as in the case of the Moon; they range from 120 to 200 for all five sets of data. This behavior is characteristic of a smooth surface having an abundance of small structure. For, if the slopes of the Venusian surface are steeper than those of the Moon (as indicated by the lower values of K), then diffraction effects may offset the basic wavelength dependence more than in the case of the lunar surface.

Comparison between the lunar and Venusian surface is best made for the mutually closest wavelengths available. This is the case for the lunar data measured at 68 cm [Evans and Pettengill, 1963] and the Venusian data obtained at 70 cm [Dyce, Pettengill, and Sanchez, 1965], yielding the values $R = 85$, $K = 0.95$ (fig. 5) and $R = 120$, $K = 1.0$ (fig. 7) respectively. Comparing the values of R, it follows that the surface of Venus is smoother than that of the Moon. This is also confirmed by the data of Klemperer, Ochs, and Bowles [1964], measured at a wavelength of 6 m, which yield $R = 165$ for the Moon (fig. 5) and $R = 200$ for Venus. On the other hand, the smaller values of K at the shorter wavelengths (0.1 at $\lambda = 23$ cm and 0.4 at $\lambda = 12.5$ cm for Venus as against 3.6 at $\lambda = 3.6$ cm for the Moon) indicate steeper slopes for Venus. Recalling that "smoother" refers to the standard deviation of the surface, whereas its slopes are determined by the correlation function, the above results indicate that small structure is present to a larger degree on Venus than on the Moon.

5. Conclusions

The expression (18) for the mean power backscattered from the rough surface of the Moon or a planet was derived under certain assumptions stated in section 2. The formula is in very good agreement with the measured curves at five different frequencies in the case of the Moon; for the data available from Venus the agreement is also good. Comparison of the two sets of curves shows that Venus must be smoother than the Moon, but has more small structure.

The limitations of (18) are primarily given by the quantitatively unknown part of the wavelength dependence of the parameters R and K, as explained in more detail in section 2. Although (18) is evidently the correct functional dependence, the numerical values of the parameters R and K should therefore be used with caution when drawing conclusions on the properties of the surface that determine R and K.

The other limitations appear less important. The fact that (6) assumes a stationary process (although the statistical characteristics of the lunar surface will vary around the illuminated ring) does not appear detrimental to the good agreement shown in figure 5, although in the case of Venus a small irregularity appears that may well be due to this point. Similarly, the assumption of perfect conductivity is, for the reasons given in section 2, practically immaterial for the calculation of the relative mean power backscattered at various angles of incidence. The conductivity will, however, significantly affect the depolarization of the backscattered radiation; this is an altogether different problem that we have not investigated here.

6. References

Beckmann, P. (1965a), Scattering by composite rough surfaces, Proc. IEEE **53**, No. 8, 1012–1015.

Beckmann, P. (1965b), Shadowing of random rough surfaces, IEEE Trans. Ant. Prop. **AP-13**, No. 3, 384–388.

Beckmann, P., and A. Spizzichino (1963), The Scattering of Electromagnetic Waves from Rough Surfaces (Pergamon Press, London, and Macmillan Co., New York).

Carpenter, R. L. (1964), Study of Venus by CW radar, Astron. J. **69**, 2–11.

Carpenter, R. L. (1965), Paper read before the American Astronomical Society Meeting, Lexington, Kentucky, March 14–17, Sky and Telescope **29**, 356–357.

Davis, J. R., and D. C. Rohlfs (1964), Lunar radio-reflection properties at decameter wavelengths, J. Geophys. Res. **69**, 3257–3262.

Dyce, R. B., G. H. Pettengill, and A. D. Sanchez (1965), Radar reflectivity of Venus and Mercury, Paper CS–2, Spring Meeting URSI-USNC, Washington, D.C.

Evans, J. V. (1965a), Radar studies of the Moon, MIT Lincoln Lab, Report DS–1423.

Evans, J. V. (1965b), Private communication reported by Pettengill [1965].

Evans, J. V., and G. H. Pettengill (1963), The scattering behavior of the Moon at wavelengths of 3.6, 68 and 784 centimeters, J. Geophys. Res. **68**, 423–446.

Hayre, H. S. (1965), Random surface with correlated large and small scale roughness, Paper 2–1–4, Spring Meeting URSI-USNC, Washington, D.C.

Klemperer, W. K. (1965), The angular scattering law for the Moon at 6 meters wavelength, J. Geophys. Res. **70**.

Klemperer, W. K., G. R. Ochs, and K. L. Bowles (1964), Radar echoes from Venus at 50 Mc/s, Astron. J. **69**, 22–28.

Kotelnikov, V. A. (1965), Radar observations of Venus in the Soviet Union in 1964, Symposium on Lunar and Planetary Surfaces, Arecibo, Puerto Rico, May 1965. The paper was based on previous publications in Radiotekhn. i Elektron., No. 11, 1962; Doklady Akad. Nauk SSSR **151**, No. 3, 1963; Priroda, No. 9, 1964.

Lynn, V. L., M. D. Sohigian, and E. A. Crocker (1964), Radar observations of the Moon at a wavelength of 8.6 millimeters, J. Geophys. Res. **69**, 781–783.

Muhleman, D. O. (1965), private communication.

7. Additional Related Reference

Pettengill, G. H. (1965), A review of radar studies of planetary surfaces, Symposium on Lunar and Planetary Surfaces, Arecibo, Puerto Rico, May.

T. Hagfors: Doesn't the theory presented here grossly overestimate the effects of shadowing, since the shadowed regions would not be inclined favorably for reflection anyway?

Answer: No; cf. sec III and IV of Beckmann [1965b].

R. M. Goldstein: It seems as though the returned power does not go to zero at the limb, in your expression.

Answer: It goes to zero, cf. (14) for $\theta \rightarrow \pi/2$.

(Paper 69D12–621)

A Note on the Radio Reflectivity of the Lunar Surface

A. Giraud

National Center of Telecommunicational Studies, CDS Department, Issy les Moulineaux (Seine)

To the extent that scattering phenomena can put boundary conditions on properties of the surface, the results obtained by the use of radar have provided less information on the lunar surface than the passive radio observations. Where the latter have given information such as on the refractive index or the thermal resistivity, the interpretation of the lunar radar echoes has dealt principally with the character of the geometry of the reflected surface. Once this aspect is established, it is possible to obtain the reflection coefficient at normal incidence, given by Fresnel's formula,

$$\frac{1-\sqrt{K'+iK''}}{1+\sqrt{K'+iK''}} \tag{1}$$

where K' and K'' are the real and imaginary parts of the complex relative permittivity.

In this way one finds $K' \simeq 2.7$ at decimeter wavelengths. The same coefficient of reflectivity obtained at centimeter wavelengths by Russian radio astronomers, through the surface emissivity and Kirchhoff's Law, give us $K' \simeq 1.5$. This difference between the properties of the lunar surface was attributed to the greater penetration of the longer waves.

In this study we propose to explain such a variation of the coefficient of reflectivity with wavelength, by using only radar data. We will quantitatively explain this variation by the use of a model where the lunar surface does not consist of abrupt discontinuities—where the reflective properties may be explained by (1) at wavelengths greater than a few meters.

1. The Spectra of the Lunar Reflectivity at Short Wavelengths

1.1. General

The published results of lunar radar observations range from wavelengths of about 1 cm to more than 10 m. They show a progressive change in the mechanism of reflection, being diffused at millimeter wavelengths and semitransparent at decameter wavelengths (fig. 1). At the same time, the fraction of the returned energy, or the effective scattering cross section σ, seems to increase by a factor of the order of two (fig. 2) between 10 cm and 10 m. We can write

$$\sigma = \pi a^2 r g, \tag{2}$$

Where a is the radius, g represents the "gain" due to the geometric characteristics of the surface, and r is the mean "albedo" corresponding to the intrinsic electromagnetic properties of the material responsible for it.

For the extreme cases of a perfectly smooth sphere and of one completely diffused (according to Lambert's law), the factors r and g are independent. Let us assume that the constituents have the same dielectric constant K to a depth much larger than the wavelengths in use.

In the first case we have

$$\sigma_{\text{smooth}} = \pi a^2 |R|^2, \tag{3}$$

where R is Fresnel's coefficient for normal incident given by (1). For $K=3$, for example, we have

$$\sigma_{\text{smooth}} = 0.072\pi a^2. \tag{4}$$

In the second case,

$$\sigma_{\text{Lambert}} = \frac{8}{3}\pi a^2 |\bar{R}|^2, \tag{5}$$

where $|\bar{R}|$ represents a mean reflection coefficient averaged for all incident angles and all polarizations. It is possible to show numerically that $|\bar{R}|^2 = 0.125$; therefore

$$\sigma_{\text{Lambert}} = 0.33\pi a^2. \tag{6}$$

As the wavelength becomes longer, the effective lunar cross section, instead of increasing, decreases by a factor of 4 or 5 at the same time that the specular